BIOCHEMISTRY
including biophysical chemistry & molecular biology

Article

pubs.acs.org/biochemistry

X-ray Structures of Magnesium and Manganese Complexes with the N-Terminal Domain of Calmodulin: Insights into the Mechanism and Specificity of Metal Ion Binding to an EF-Hand

F. Timur Senguen and Zenon Grabarek*

Boston Biomedical Research Institute, Watertown, Massachusetts 02472, United States

Supporting Information

ABSTRACT: Calmodulin (CaM), a member of the EF-hand superfamily, regulates many aspects of cell function by responding specifically to micromolar concentrations of Ca^{2+} in the presence of an ~1000-fold higher concentration of cellular Mg^{2+}. To explain the structural basis of metal ion binding specificity, we have determined the X-ray structures of the N-terminal domain of calmodulin (N-CaM) in complexes with Mg^{2+}, Mn^{2+}, and Zn^{2+}. In contrast to Ca^{2+}, which induces domain opening in CaM, octahedrally coordinated Mg^{2+} and Mn^{2+} stabilize the closed-domain, apo-like conformation, while tetrahedrally coordinated Zn^{2+} ions bind at the protein surface and do not compete with Ca^{2+}. The relative positions of bound Mg^{2+} and Mn^{2+} within the EF-hand loops are similar to those of Ca^{2+}; however, the Glu side chain at position 12 of the loop, whose bidentate interaction with Ca^{2+} is critical for domain opening, does not bind directly to either Mn^{2+} or Mg^{2+}, and the vacant ligand position is occupied by a water molecule. We conclude that this critical interaction is prevented by specific stereochemical constraints imposed on the ligands by the EF-hand β-scaffold. The structures suggest that Mg^{2+} contributes to the switching off of calmodulin activity and possibly other EF-hand proteins at the resting levels of Ca^{2+}. The Mg^{2+}-bound N-CaM structure also provides a unique view of a transiently bound hydrated metal ion and suggests a role for the hydration water in the metal-induced conformational change.

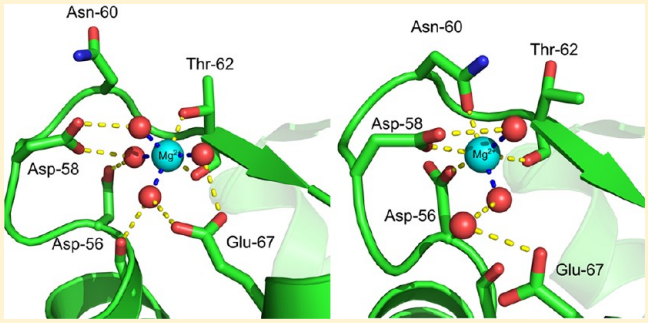

Transient spikes in the free Ca^{2+} concentration activate the function of excitable cells such as myocytes and neurons and regulate a broad range of processes in virtually all cells.[1−3] In the resting state, the concentration of free Ca^{2+} is ~0.1 μM and may increase ~100-fold upon cell activation. In contrast, the concentration of free Mg^{2+} is much higher and remains at a nearly constant level of ~1.0 mM.[4] Thus, Ca^{2+} signaling occurs in the presence of a large excess of chemically similar divalent cation Mg^{2+}. Although Mg^{2+} is generally considered not to play a regulatory function, large fluxes of Mg^{2+} through the cell membrane can be elicited upon hormonal stimulation in situ,[5−9] which suggests that the free Mg^{2+} concentration in cells is tightly regulated. Significant changes in the intracellular free Mg^{2+} concentration may occur in some pathological states such as dietary magnesium deficiency[10] or ischemia.[11] Several observations point to an antagonistic role of Mg^{2+} with respect to Ca^{2+} in cell function; however, the underlying mechanisms are not well understood. Recently, we put forward a hypothesis that altered Ca^{2+} regulation may be an underlying cause of some pathological states attributed to magnesium deficiency.[12] This work is an attempt at further exploration of this possibility through a detailed structural analysis of the interaction of Mg^{2+} with the key Ca^{2+} sensor protein calmodulin (CaM).

Calmodulin is a member of the EF-hand superfamily of Ca^{2+}-binding proteins that function as intracellular receptors of Ca^{2+} signals. These proteins change their conformation upon binding Ca^{2+}, the property that allows them to regulate the activity of various enzymes in a Ca^{2+}-dependent manner.[13−15] Many EF-hand proteins also bind Mg^{2+} with sufficient affinity to render them fully or partially filled with Mg^{2+} at the resting Ca^{2+} levels. Thus, the key question is how these proteins respond specifically to Ca^{2+} signals in the presence of an ~1000-fold excess of Mg^{2+}. Such remarkable functional specificity requires not only a metal ion discrimination based on the binding affinity but also different structural responses to Ca^{2+} binding versus Mg^{2+} binding. Even though the Ca^{2+}-binding sites in CaM are considered Ca^{2+}-specific, they have sufficient affinity for Mg^{2+} to be partially occupied by Mg^{2+} (possibly as much as 50% in the N-terminal domain) at the resting intracellular Ca^{2+} concentrations[16−18] (reviewed in ref 12). The Ca^{2+}-induced activation of CaM requires a transition from a closed-domain to an open-domain conformation in which a target-binding hydrophobic pocket is formed in each of its two domains.[19,20] Mg^{2+} ions do not induce domain opening and thus do not activate CaM,[17,21] but the structural basis for the different conformational response is not well understood.

Received: May 28, 2012
Revised: July 15, 2012
Published: July 17, 2012

The metal-coordinating ligands in the canonical EF-hand are contained within a 12-amino acid loop, flanked on both ends by α-helices.[22,23] A pair of EF-hands is required for a structurally stable functional domain. The key element of the domain is a short stretch of antiparallel β-sheet connecting the Ca^{2+}-binding loops named "EF-hand β-scaffold", which was proposed to play an important role in the Ca^{2+} binding mechanism and in the Ca^{2+}-induced conformational changes.[14,24] In the proposed model, the position of the bound metal ion is defined by the central carbonyl oxygen ligand (position $-Y$), a part of the β-scaffold. The ligands in the N-terminal part of the loop are highly mobile and fold readily around the metal ion without significant effects on the domain structure, whereas the contribution of a bidentate ligand provided by the side-chain carboxyl group of the invariant Glu reside in the C-terminal (12th) position of the loop (Glu_{12}) requires a shift of the exiting helix, which opens the domain. The bidentate Ca^{2+} coordination by Glu_{12} is critical for the domain opening,[24,25] and that interaction is different or missing in the Mg^{2+}–EF-hand protein structures. In the Mg^{2+}-bound structure of parvalbumin,[26] only one oxygen of the Glu_{12} side chain interacts with the metal (monodentate ligand), whereas in the structure of calbindin D9k (S100G), Glu_{12} does not contact Mg^{2+} at all[27] and the vacant coordinating position is occupied by H_2O (reviewed in ref 12). Neither protein undergoes a large conformational change upon Ca^{2+} binding, so it is not possible to make inferences from these structures with respect to CaM. On the basis of their NMR studies, Malmendal and colleagues concluded that Glu_{12} does not contribute to Mg^{2+} binding in the N-terminal domain of CaM,[17,18] consistent with the closed-domain conformation of the Mg^{2+}–CaM complex.[28] However, the structural basis for that difference is not clear.

Here we report X-ray structures of the N-terminal domain of calmodulin (N-CaM) in complexes with three divalent metal ions: Mg^{2+}, Mn^{2+}, and Zn^{2+}. The hexacoordinated Mg^{2+} and Mn^{2+} are bound within the EF-loops, whereas the tetracoordinated Zn^{2+} is found only at the interface between N-CaM monomers in the crystal lattice. In these structures, N-CaM has a closed-domain apo-like conformation. Characteristically, the last ligand of the Ca^{2+}-binding loop (Glu_{12}) is not involved in Mg^{2+} or Mn^{2+} binding, which explains the lack of domain opening and CaM activation by these metal ions. Although like Ca^{2+}, both Mg^{2+} and Mn^{2+} stabilize the N-CaM structure against thermal and urea-induced unfolding, the stabilized structures are different. Cumulatively, the presented structures allow us to define the determinants of metal ion specificity in N-CaM. Unexpectedly, one of the structures provides a unique view of a bound hydrated Mg^{2+} and suggests that tightly coordinated water molecules may be important for the metal-induced conformational transition.

MATERIALS AND METHODS

Protein Expression, Purification, and Decalcification. The N-terminal domain of human CaM (residues 1–79) cloned in the pAED4 vector[29] was expressed and purified in a similar manner as we previously described for wild-type CaM.[20] Briefly, transformed Rosetta cells (Novagen) were grown in 1 L of LB at 37 °C. Protein overexpression was induced with 0.1 mM isopropyl 1-thio-β-D-galactopyranoside when OD_{600} reached 0.8–1.0, and the culture was incubated for 3 h at 37 °C. Cells were harvested via centrifugation (4500 rpm for 15 min at 4 °C) and lysed by freezing and thawing of the pellet (three cycles) suspended in lysis buffer [50 mM Tris (pH 8.0), 1 mM EDTA, and 0.1 mM PMSF]. Cell debris was removed via centrifugation (16000 rpm for 20 min at 4 °C), and the supernatant was brought to 35% saturation of $(NH_4)_2SO_4$ and centrifuged again. The supernatant was filtered through a syringe filter (Whatman, 0.2 μm PVDF with GMF) and after addition of 4 mM $CaCl_2$ applied to a fast flow Phenyl-sepharose column. The column was then washed with high-salt [1 M NaCl, 50 mM Tris (pH 8.0), and 2 mM $CaCl_2$], low-salt [0.1 M NaCl, 50 mM Tris (pH 8.0), and 2 mM $CaCl_2$], and medium-salt [0.3 M NaCl, 50 mM Tris (pH 8.0), and 2 mM $CaCl_2$] buffers. Purified protein was eluted with 2 mM EDTA [0.3 M NaCl and 50 mM Tris (pH 8.0)], and the protein-containing fractions were pooled. The combined fractions were dialyzed against low-salt DEAE buffer [50 mM NaCl and 20 mM BisTris (pH 6.0)] and purified on a DEAE column with a salt gradient (50 to 500 mM NaCl). Purified N-CaM was dialyzed against 2 mM NH_4HCO_3 and lyophilized. For crystallization, lyophilized protein was dissolved in a minimal amount of 2 mM Hepes (pH 7.5) and dialyzed against EDTA buffer (20 mM EDTA with 100 mM NaCl) to ensure decalcification, followed by dialysis against decreasing concentrations of EGTA (20 and 0.5 mM EGTA) to maintain a calcium free environment.

Isothermal Titration Calorimetry. Metal binding constants were determined via ITC using a VP-ITC calorimeter (MicroCal) and the data analyzed with Origin 7 (MicroCal).[30] Decalcified N-CaM samples were dialyzed against ITC buffer [50 mM Tris-cacodylate (pH 6.5) and 100 mM KCl] and diluted to 20, 20, and 150 μM for titration with $CaCl_2$, $MnCl_2$, and $MgCl_2$, respectively. Each protein sample was degassed and immediately used for titration at 22 °C. A series of 10 μL aliquots with a 20-fold molar excess of metal relative to total protein concentration were added, and the heat due to binding of a metal ion to N-CaM was measured calorimetrically. In each case, a total of 300 μL of metal ion solution was added. Each data set was integrated and the resulting plot fit with a single-set-of-sites model using a nonlinear least-squares minimization algorithm. The fit parameters were used to calculate the dissociation constant, K_d, and enthalpy changes, ΔH, due to the binding of Ca^{2+}, Mn^{2+}, and Mg^{2+} ions to N-CaM.

Thermal Unfolding Monitored by Far-UV Circular Dichroism Spectroscopy. Thermal denaturation curves of N-CaM were obtained using an AVIV 62DS CD spectrometer. Protein samples (5 μM) in CD buffer [3 M urea and 10 mM Hepes (pH 7.0)] were titrated with $CaCl_2$ (0–1 mM), $MnCl_2$ (0–10 mM), or $MgCl_2$ (0–10 mM). Sodium chloride was added as necessary to maintain a constant ionic strength of 100 mM. N-CaM samples were denatured from 15 to 95 °C in 1 °C increments (30 s equilibration time), and the ellipticity at 222 nm was averaged for 5 s and recorded. The thermal unfolding curves were fit to determine the melting temperature, T_m, and heat of unfolding, ΔH, as we described previously.[31]

Protein Crystallization. All crystals were grown at room temperature using the hanging drop vapor diffusion method with 2 μL drops over reservoirs containing 250 μL of crystallization solution. N-CaM crystals containing Mn^{2+}/Zn^{2+} and Mg^{2+}/Zn^{2+} metal ions were grown from 100 mM Tris-cacodylate (pH 6.5), 25 mM $ZnCl_2$, 16% PEG8000, 100 mM $MnCl_2$ or $MgCl_2$, and 20% ethylene glycol. Crystal formation under these conditions was complete within 1 day. Crystals containing only Mg^{2+} were grown from 20 mM Tris-cacodylate (pH 7.0), 32% PEG8000, 25 mM magnesium acetate, 50 mM KCl, and 25% ethylene glycol. After equilibration for 2 days, the

dx.doi.org/10.1021/bi300698h | Biochemistry 2012, 51, 6182–6194

Table 1. Structure Determination of N-CaM−Metal Ion Complexes[a]

	Mg/Zn−N-CaM	Mg−N-CaM	Mn/Zn−N-CaM	
Data Collection				
wavelength (Å)	1.0750	1.0750	1.0750	1.7587
space group	$P4_32_12$	$P1$	$P2_1$	
no. of molecules in the asymmetric unit	1	4	2	
cell dimensions				
a (Å)	35.30	34.44	36.29	36.32
b (Å)	35.30	43.04	35.46	35.50
c (Å)	142.94	53.69	58.34	58.39
α (deg)	90.00	68.45	90.00	90.00
β (deg)	90.00	88.62	93.12	92.79
γ (deg)	90.00	79.45	90.00	90.00
resolution (Å)	1.8	1.76	1.90	2.15
R_{merge} (%)	15.7 (59.2)[b]	7.1 (40.4)[b]	6.5 (33.5)[b]	6.9 (30.5)[b]
$I/\sigma(I)$	18.3 (8.4)[b]	15.6 (2.7)[b]	28.7 (6.2)[b]	26.6 (4.8)[b]
completeness (%)	100.0 (100.0)[b]	95.6 (87.5)[b]	100 (99.9)[b]	99.7 (97.7)[b]
redundancy	27.4 (26.4)[b]	4.0 (3.3)[b]	8.2 (3.7)[b]	3.8 (3.0)[b]
Refinement				
no. of unique reflections	9179	27732	11882	8287
R_{work}	0.2023	0.198	0.204	
R_{free}	0.228	0.233	0.234	
no. of atoms				
protein	575	2371	1150	
ligand/ion	9	10	10	
water	68	147	72	
B factor				
protein	37.2	36.39	39.56	
ligand/ion	33.04	26.01	40.88	
water	50	35.65	41.94	
rmsd				
bond lengths (Å)	0.008	0.009	0.017	
bond angles (deg)	1.302	0.877	1.218	
Ramachandran plot (%)				
favorable region	98.7	99.34	97.93	
allowed region	1.3	0.66	2.07	
disallowed region	0	0	0	
PDB entry	3UCY	3UCW	3UCT	

[a]All data sets were collected at NSLS beamline X29. [b]Outer resolution shell (1.86−1.80, 1.82−1.76, 1.97−1.90, and 2.23−2.15 Å, from left to right, respectively).

clear drop was microseeded. All crystals were frozen in liquid nitrogen directly from the crystallization solution.

X-ray Data Collection, Structure Solution, and Refinement. Data for all crystals were collected at beamline X29 of the National Synchrotron Light Source (Brookhaven, NY). A complete data set was collected for each crystal at 100 K at a wavelength of 1.0750 Å. For the Mn/Zn−N-CaM crystal, an additional data set was collected at 1.7587 Å where the anomalous signal due to Mn is stronger than the anomalous signal due to Zn. Reflections were indexed and integrated with DENZO and scaled with SCALEPACK.[32] Data from SCALEPACK were then converted into MTZ format with structure factors using ImportScaled and ctruncate, which are included in the CCP4 program suite.[33]

SAD phases were determined for Mg/Zn−N-CaM and Mn/Zn−N-CaM crystals using the AutoSol module in the Phenix suite,[34] using the anomalous signal due to the presence of Zn. The Mg−N-CaM crystal structure was determined using molecular replacement with Phaser-MR and a previously reported apo CaM structure [Protein Data Bank (PDB) 2PQ3]. Electron density maps were improved by creating iterative build composite omit maps using AutoBuild (Phenix).[35] The initial models used for refinement were also created using AutoBuild with the appropriate sequence file for the N-terminal domain of calmodulin.

Initial automatic structural refinement was performed with phenix.refine. Metal ions and cacodylate groups were added manually in Coot[36] and ligand restraints produced using ReadySet (Phenix). Following the initial cycle of automatic refinement, several cycles of manual refinement in Coot as well as automatic refinement with phenix.refine and/or refmac5 were performed until R_{work} and R_{free} had reached acceptable values. Validation of the structure was performed using the Comprehensive Validation option in the Phenix program suite, as well as PROCHECK. Model statistics for each refined crystal structure are listed in Table 1.

RESULTS

While both domains of CaM reportedly bind Mg^{2+}, the binding to the N-domain is sufficiently strong to significantly affect the regulatory function of CaM under physiological conditions.[17,18,37,38] Therefore, our goal was to obtain the high-

dx.doi.org/10.1021/bi300698h | Biochemistry 2012, 51, 6182−6194

resolution structure of the Mg^{2+}−N-CaM complex. A search for the crystallization conditions using Hampton Research Crystal Screens I and II yielded tetragonal crystals (space group $P4_32_12$), which contained also Zn^{2+} ions in addition to Mg^{2+}. Similar crystals of N-CaM obtained in the presence of Zn^{2+} only have been previously reported by Warren et al.[39] Upon searching further, we have obtained triclinic crystals of N-CaM in the presence of Mg^{2+} only. The third structure is that of a monoclinic crystal of the Mn^{2+}−N-CaM complex also obtained in the presence of Zn^{2+}. The three metal ions used in this study have similar ionic radii: 0.72 Å for Mg^{2+}, 0.67 Å for Mn^{2+}, and 0.74 Å for Zn^{2+} in the octahedral coordination and 0.60 Å for Zn^{2+} in its more common tetrahedral coordination.[40] Thus, these metal ions are significantly smaller than Ca^{2+} ions, whose ionic radius is 1.00 Å in the octahedral coordination and 1.06 Å in the pentagonal bipyramid geometry typical for Ca^{2+} complexes with EF-hand proteins. Mg^{2+} and Mn^{2+} prefer octahedral ligand geometry, whereas Zn^{2+} has a preference for tetrahedral coordination. The important difference between Mg^{2+} and Mn^{2+} is that the latter binds N-CaM much more strongly (Table 2 and Figure 1 of the Supporting Information).

Table 2. Thermodynamic Parameters of the Binding of Metal to N-CaM Determined by Isothermal Titration Calorimetry

	Ca^{2+}	Mn^{2+}	Mg^{2+}
no. of sites	2.1 ± 0.1	2.0 ± 0.1	1.8 ± 0.2
K_d (μM)	5.6 ± 0.1	13 ± 2	450 ± 10
ΔH (kcal/mol)	1.68 ± 0.06	3.8 ± 0.3	10 ± 1
ΔS (cal mol^{-1} K^{-1})	29.7	34.9	48.7

In all the structures described here, N-CaM has a closed-domain apo-like conformation, consistent with the fact that none of the three metal ions is able to activate CaM. The structures are described in more detail below.

Tetragonal Mg/Zn−N-CaM Crystals. The Mg^{2+}−N-CaM complex forms tetragonal crystals in the presence of Zn^{2+} and sodium dimethylarsenate (cacodylate). The structure was determined by molecular replacement using the coordinates of the N-CaM structure obtained in the presence of Zn^{2+} only[39](PDB entry 2PQ3). Both Ca^{2+}-binding loops of N-CaM in the Mg/Zn−N-CaM crystal contain an octahedrally coordinated metal ion. In site II, the metal oxygen bond lengths (2.18 ± 0.11 Å) are consistent with Mg^{2+}.[41,42] However, in site I, the metal−oxygen bonds (2.41 ± 0.09 Å) are outside the accepted range for Mg^{2+}. The possible candidates are Ca^{2+} or Na^+ ions, for which the average bond lengths found in high-resolution protein structures fall in the same range of 2.35−2.45 Å.[42] Calcium is a likely contaminant because of its high affinity for N-CaM; however, modeling the electron density as Ca^{2+} resulted in a large negative peak in the $F_o - F_c$ electron density map. Furthermore, the octahedral ligand geometry of the bound metal is inconsistent with the pentagonal bipyramid geometry of Ca^{2+} coordination found in all published CaM structures. Thus, we have concluded that Na^+ is most likely the metal bound at site I. While a relatively strong binding of Na^+ to CaM (K_a = 230 M^{-1}) has been detected with ^{23}Na NMR,[43] it is surprising that Mg^{2+} ions did not outcompete Na^+ at this position in the crystal. A significant restriction of the loop conformation due to an interaction with a symmetry-related molecule might be responsible. The O^{δ} atoms of Asp22 and Asp24 not only coordinate Na^+ but also interact with one of the Zn^{2+} ions. The metal ion cluster is further stabilized by the oxygen atoms of dimethylarsenate, which provides a bridge between the two metal ions as well as the same cluster of a symmetry-related molecule.[39] This leads us to postulate that the absence of Mg^{2+} in site I results from the unfavorable position of Asp22 and Asp24 side chains due to the interaction with Zn^{2+}.

The Mg^{2+} ion bound in site II is octahedrally coordinated by O^{δ} atoms of Asp56, Asp58, and Asn60 and the carbonyl oxygen of Thr62 (Figure 1A). The two remaining coordinating positions are occupied by water molecules. The Glu residue at position 12 of the loop (Glu67), which provides bidentate coordination to Ca^{2+}, does not interact directly with Mg^{2+} ion. The lack of this interaction critical for the Ca^{2+}-induced domain opening[24,25] is, apparently, the reason for the closed-domain conformation of N-CaM in this complex. Importantly, in this structure, Mg^{2+} occupies the same position as Ca^{2+} by directly engaging four of the six ligands that typically are involved in Ca^{2+} coordination. Thus, the structure indicates that Mg^{2+} can be a direct competitor with respect to Ca^{2+} for site II of CaM depending upon their respective concentrations.

Triclinic Mg−N-CaM Crystals. To resolve the issue of Mg^{2+} binding to site I, we have crystallized N-CaM in the presence of Mg^{2+} as the sole divalent metal ion. The structure of the Mg^{2+}−N-CaM complex reveals three different modes of interaction of Mg^{2+} with CaM. Two ions are coordinated to the ligands provided by the Ca^{2+}-binding loops, whereas the third ion is coordinated by the side-chain carboxyls from adjacent molecules in the crystal lattice. At 1.76 Å resolution (Table 1), all the bound Mg^{2+} ions and the interacting ligands, including the tightly coordinated water molecules, are well represented in the electron density map (Figure 1B). The average temperature factor for the bound Mg^{2+} is 26.0 ± 4.8 Å^2 (range of 20.4−33.8 Å^2). The asymmetric unit contains four molecules of N-CaM arranged in two pairs. Within each pair, the molecules are positioned back to back (Figure 2). This interaction is stabilized by multiple contacts between the helices of site II (helices C and D) and the Mg^{2+} ion coordinated by the side chains of Asp64, the residue at position 9 of loop II. The back-to-back interaction of the N-CaM monomers apparently restricts the movement of the helices in EF-hand II, which has some important structural consequences. Each monomer of the Mg^{2+}-bound N-CaM has a closed-domain conformation similar to that found in the apo structure; however, there are key differences in the position of the helices in site II (see below). The coordination geometry of all Mg^{2+} ions in this structure is octahedral. The metal−oxygen bond lengths are in excellent agreement with the expected Mg^{2+}−oxygen bond length. In site I, four of the six coordinating positions of the bound Mg^{2+} are occupied by the protein ligands that are normally involved in Ca^{2+} coordination (side-chain oxygen atoms of Asp20, Asp22, and Asp24 and the carbonyl oxygen of Thr26). The two remaining coordinating positions (−X and −Z) are occupied by H_2O. The position of the bound Mg^{2+} ion is the same as that of Ca^{2+}, except that the Glu_{12} bidentate ligand (Glu31) is not engaged. Thus, this structure shows that site I of N-CaM is fully capable of coordinating the Mg^{2+} ion, and it supports our earlier conclusion that the lack of Mg^{2+} in site I of Mg/Zn−N-CaM crystals resulted from constraints on the ligands (Asp22 and Asp24) due to their simultaneous interaction with Zn^{2+}.

Unexpectedly, in site II the Mg^{2+} ion is bound in a very different manner (Figure 1B). The oxygen atom ligands contributed by the protein occupy only two of the six

dx.doi.org/10.1021/bi300698h | Biochemistry 2012, 51, 6182−6194

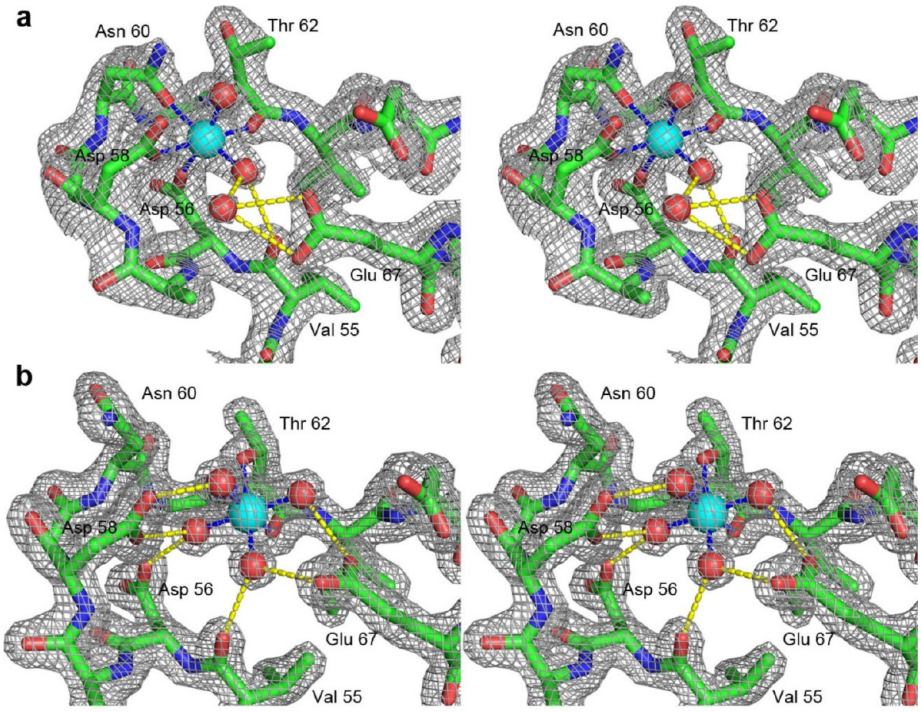

Figure 1. Two modes of interaction of Mg^{2+} with site II of N-CaM. Stereodiagrams showing $2F_o - F_c$ electron density maps contoured at 1.5σ and the corresponding atomic models for site II of N-CaM (residues 55−67). (a) "Final" state found in the tetragonal Mg/Zn−N-CaM crystals. (b) "Intermediate" state found in the Mg−N-CaM monoclinic crystal. Note the difference in the position of the metal ion (cyan spheres) and in the number of water molecules (red spheres) retained by Mg^{2+}. In the intermediate state (b), the Mg^{2+} ion is directly coordinated to N-CaM (blue lines) only via Thr62 side-chain and backbone carbonyl oxygen atoms. The four remaining coordinating positions are occupied by water molecules that make strong hydrogen bonds (yellow lines) with the side chains of Asp58, Glu67 (each contributing two oxygen atoms), the side chain of Asp56, and the backbone carbonyl atom of Val55. A transition from the initial to the final position requires the elimination of two additional water molecules from the coordination sphere of Mg^{2+}, which are replaced by direct bonds to side-chain oxygen atoms of Asp56, Asp58, and Asn60. Two water molecules complete the octahedral ligand geometry around the Mg^{2+} ion, one of which forms a hydrogen bond to Glu67 at the C-terminal position of the loop. The only metal ligand contributed by the protein that is common to the two structures is the carbonyl oxygen of Thr62 (the $-Y$ coordinating position), which belongs to the β-scaffold. All structure figures were prepared with Pymol.[71]

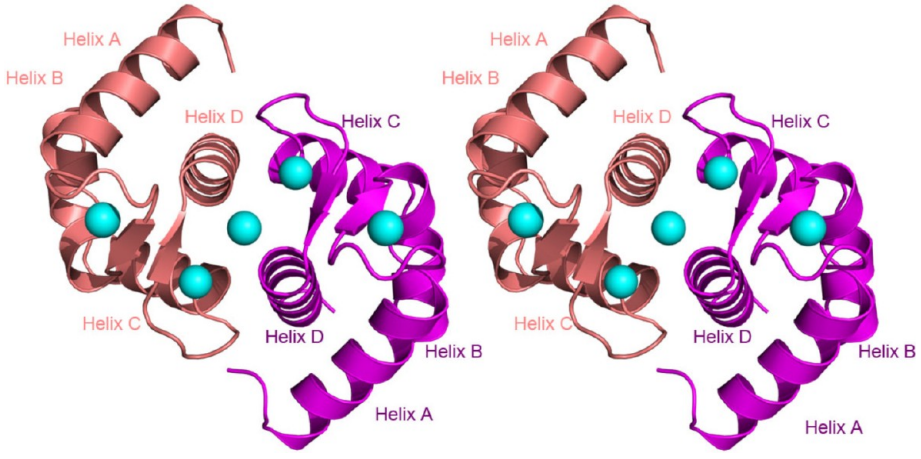

Figure 2. Stereoview of the N-CaM dimer in the monoclinic crystal of the Mg^{2+}−N-CaM complex. Mg^{2+} ions are shown as cyan spheres. Note the back-to-back interaction of N-CaM monomers involving EF-hand II and a Mg^{2+} ion coordinated by the side chains of Asp64 (the residue at position 9 of the loop). Because of the back-to-back interaction, helix C is shifted and restricted in its movement.

coordinating positions of the Mg^{2+} ion. These are the main-chain carbonyl oxygen in the $-Y$ position (Thr62), which is a part of the β-scaffold, and the O^{γ} atom of that residue. The four remaining coordinating positions are occupied by water molecules. The binding of such a highly hydrated metal ion is strongly stabilized by two-pronged hydrogen bonds of the coordinated water molecules to the side-chain carboxyl oxygen atoms of Asp58 and Glu67, the residues at positions 3 and 12 of the loop, respectively, that provide the Y and $-Z$ ligands for Ca^{2+} coordination. The entering helix (helix C) is shifted with respect to the β-scaffold in such a way that the side chain of Asp56, the first residue of the loop (the Ca^{2+} ligand at the X position), is spatially too far removed to contact the Mg^{2+} ion directly and, instead, forms a hydrogen bond with one of the

dx.doi.org/10.1021/bi300698h | *Biochemistry* 2012, 51, 6182−6194

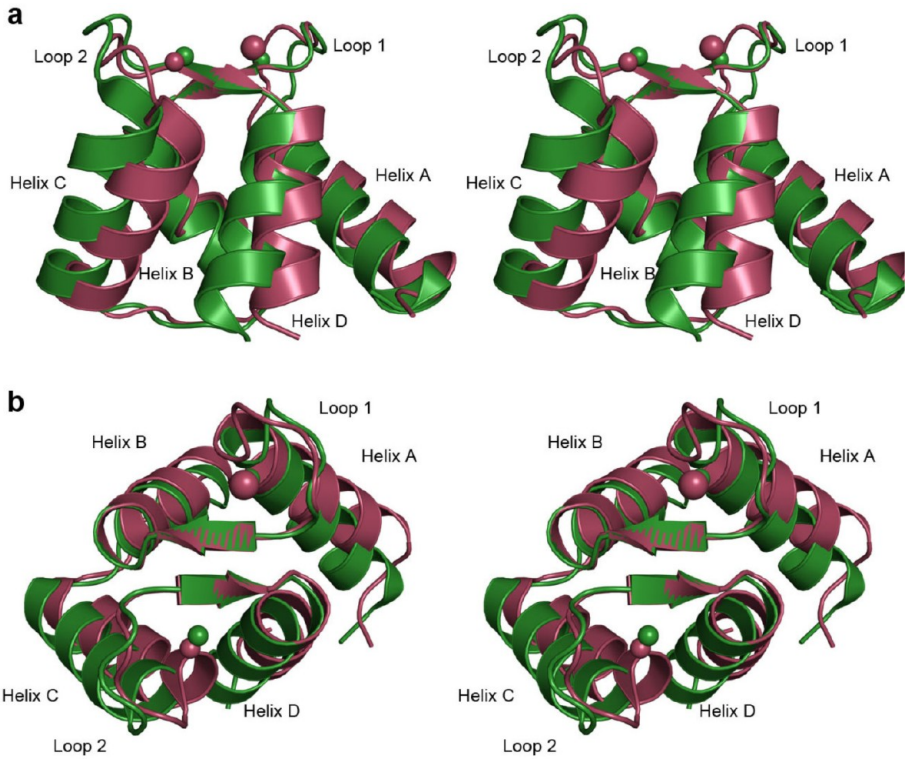

Figure 3. Comparison of the domain structure of Mg–N-CaM and Mg/Zn–N-CaM complexes. The Mg–N-CaM complex is colored green and the Mg/Zn–N-CaM complex red. Coordinates of the backbone atoms of the β-scaffold (Thr26, Ile27, Thr62, and Ile63) were used for the superimposition. Note a large shift in the position of the entering helix of site II (helix C) in the Mg^{2+}–N-CaM structure. Because of this shift, the carbonyl oxygen of Val55 is approximately in the *X* coordinating position instead of the Asp56 side chain.

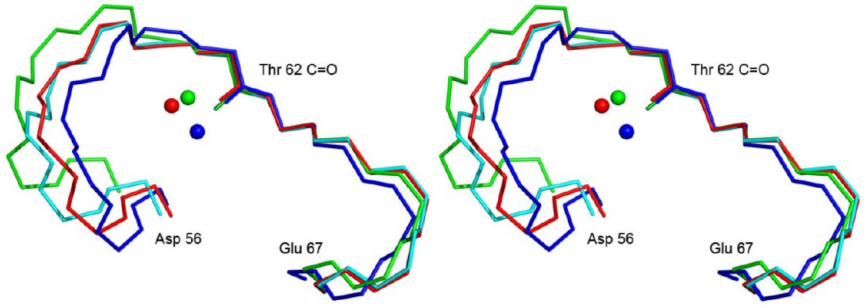

Figure 4. Fluctuation of the EF-hand loop during metal ion binding. A stereodiagram of the backbone structure of loop II of N-CaM (residues 56–67) is shown: cyan for the apo form (PDB entry 2PQ3), green for the Mg–N-CaM complex (PDB entry 3UCW) featuring the transiently bound hydrated Mg^{2+}, red for the Mg/Zn–N-CaM complex (PDB entry 3UCY) and the final position of dehydrated Mg^{2+}, and blue for the form with Ca^{2+} (PDB entry 1CLL). Note that the loop initially expands to accommodate the hydrated Mg^{2+} ion and then contracts to a conformation similar to the apo form when the H_2O molecules are replaced by loop ligands (movie in the Supporting Information). Further contraction of the loop occurs in the case of Ca^{2+} when the bidentate Glu_{12} engages in Ca^{2+} coordination. The distance between C^{α} atoms of the first and last residue of the loop are 8.6 Å (apo), 10.1 Å (hydrated Mg^{2+}), 8.1 Å (Mg^{2+}), and 6.6 Å (Ca^{2+}).

H_2O molecules coordinated to the Mg^{2+} ion. Thus, although the Mg^{2+} ion is coordinated by the ligands of the loop, it still retains most of its hydration water and has not reached the position normally occupied by Ca^{2+}. This structure appears to represent an early step in the binding of metal to an EF-hand, which was fortuitously captured because of specific intermolecular contacts in the crystal lattice, specifically the back-to-back interaction of N-CaM monomers (Figure 2) in both pairs comprising the asymmetric unit of the crystal. The ~3 Å shift of the entering helix is the key difference (Figure 3). The consequence of this shift is an expansion of the loop (Figure 4) allowing the almost fully hydrated metal ion to engage the loop ligands. We infer that the ability of the entering helix to move freely with respect to the β-scaffold is an important factor in the process of metal ion binding. The implications of this unusual mode of metal ion binding will be considered further in Discussion.

Monoclinic Mn/Zn–N-CaM Crystals. Two sets of data were collected from crystals of the Mn^{2+}/Zn^{2+}-bound form of N-CaM (Table 1). One set collected at 1.054 Å was used for determining and refining the structure, while the second set at 1.7587 Å, close to the anomalous scattering peak of Mn, was used to verify the position of the Mn^{2+} ions in the structure (Figure 5). The structure was determined by SAD phasing using anomalous signals of Mn and Zn. The monoclinic crystals (space group $P2_1$) contain two N-CaM molecules in the

dx.doi.org/10.1021/bi300698h | *Biochemistry* 2012, 51, 6182–6194

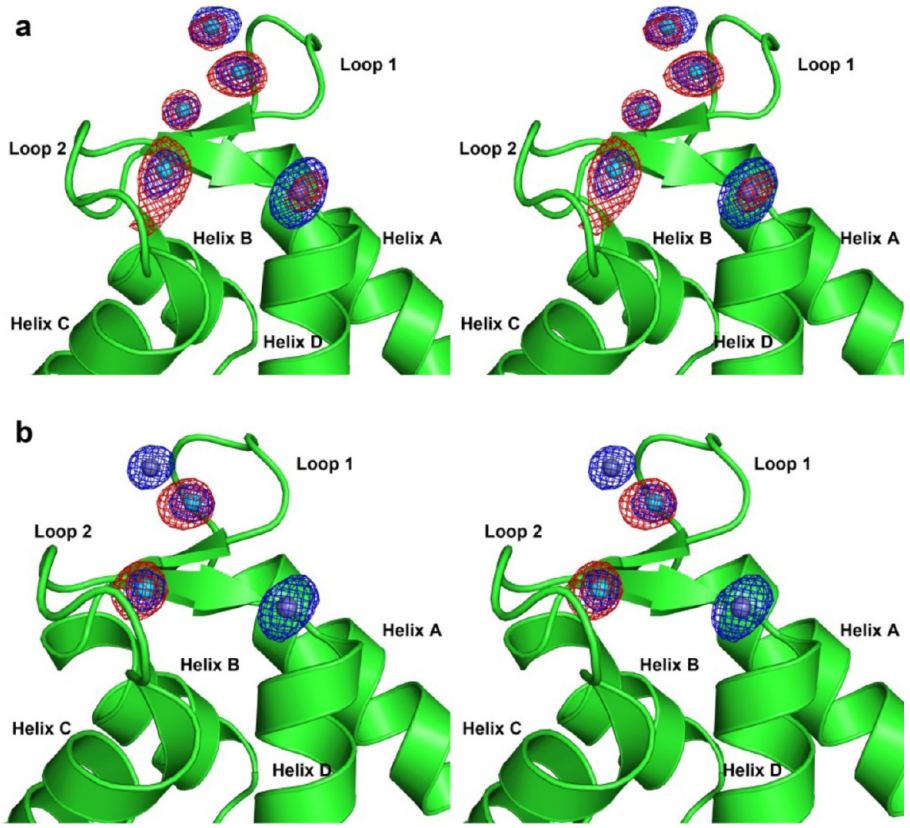

Figure 5. Identification of the bound Mn^{2+} and Zn^{2+} based on anomalous X-ray scattering. The data were recorded at two wavelengths, 1.0750 Å (blue) and 1.7587 Å (red). The f'' value for Zn^{2+} ions (dark blue spheres) is ~3-fold larger at the shorter wavelength when compared to that at the longer wavelength (2.83e and 0.92e, respectively), whereas the opposite is the case for Mn^{2+} ions (cyan spheres) (1.59e and 3.4e, respectively). (a) Chain A in which four Mn^{2+} ions and one Zn^{2+} ion are coordinated to the metal binding loops. (b) Chain B that binds one Mn^{2+} ion and one Zn^{2+} ions each in loops 1 and 2. Contours for the maps are 6.0σ with a 4.0 Å cutoff around the metal. Sphere radii are reduced to 0.5 Å for both Mn^{2+} and Zn^{2+} to improve visibility.

asymmetric unit. Both chains are in the closed-domain conformation and contain Mn^{2+} ion in each EF-hand loop with identical octahedral ligand geometry. In loop 1, Asp20 provides an axial ligand (X position) to the Mn^{2+} complex via O^{δ} with the opposite axial position ($-X$) occupied by a water molecule. The O^{δ} atoms of Asp22 and Asp24 provide two equatorial ligands with the backbone carbonyl oxygen atom of Thr26 and a water molecule completing the octahedral ligand geometry. The loop 2 configuration around the second Mn^{2+} ion is similar. One of the water molecules and the Asp58 O^{δ} atom comprise the axial ligands, while the second water molecule, the O^{δ} atoms of Asp56 and Asn60, and the carbonyl oxygen atom of Thr62 form the equatorial plane of Mn^{2+} ligation. Like in the Mg^{2+}−N-CaM complexes, the Glu_{12} residues in the $-Y$ coordinating position (Glu31 in site I and Glu67 in site II) do not interact with Mn^{2+} ion. In chain A, one of the O^{ϵ} atoms of this residue coordinates to the exogenous Mn^{2+} ion exclusive to chain A while the other O^{ϵ} atom forms a hydrogen bonding network to the Mn^{2+} ion in loop 1 via a two-water bridge. Alternatively, in chain B, one of the Glu31 O^{ϵ} atoms forms an indirect bond to the Mn^{2+} ion in loop 1 via a water bridge involving only a single water molecule.

In addition to the Mn^{2+} ions, Zn^{2+} ions from the crystallization milieu were also present, as identified from the anomalous X-ray scattering signal (Figure 5). The structure presented here includes four Zn^{2+} ions, all of which bind at the interface between N-CaM monomers in a tetrahedral geometry. Two of the Zn^{2+} ions are coordinated by Asp64 and Glu67 on the modeled chains and Glu7 and Glu11 on the symmetry-related molecules. The third Zn^{2+} binds to chain B, residues Asp50 and Glu54, and their symmetry counterparts. The final Zn^{2+} ion binds on the outside of loop 1 of chain B to two of the same residues that bind Mn^{2+}, Asp22 and Asp24, but via the alternative O^{δ} atoms and the O^{ϵ} atom of the Glu45 residue on chain A.

It is striking that none of the Zn^{2+} ions are bound to the Ca^{2+}-binding loops of N-CaM in a position normally occupied by Ca^{2+}. This, in principle, could be related to the presence of competing Mn^{2+} in the Mn/Zn−N-CaM crystals or Mg^{2+} in the Mg/Zn−N-CaM crystals described above. However, Zn^{2+} was found not to bind at the Ca^{2+}-binding sites of N-CaM even in the absence of competing ions.[39] A similar observation was reported for the interaction of the S100 protein with Zn^{2+}.[44] This is surprising in view of the fact that binding of Zn^{2+} to low-molecular weight ligands such as EDTA is several orders of magnitude stronger than that of Mg^{2+}, Ca^{2+}, or even Mn^{2+}. According to the Irving−Williams series,[45] which compares the stability of various complexes formed by the transition metals, binding of Zn^{2+} to most ligands should be at least equal to or significantly stronger than that of Mn^{2+}. This rule is clearly not applicable to the EF-hand Ca^{2+}-binding sites. A comparison of the N-CaM crystals obtained in the presence of Zn^{2+} with and without Mn^{2+} reveals a competition between these metals for the auxiliary sites located at the interface between N-CaM

dx.doi.org/10.1021/bi300698h | *Biochemistry* 2012, 51, 6182−6194

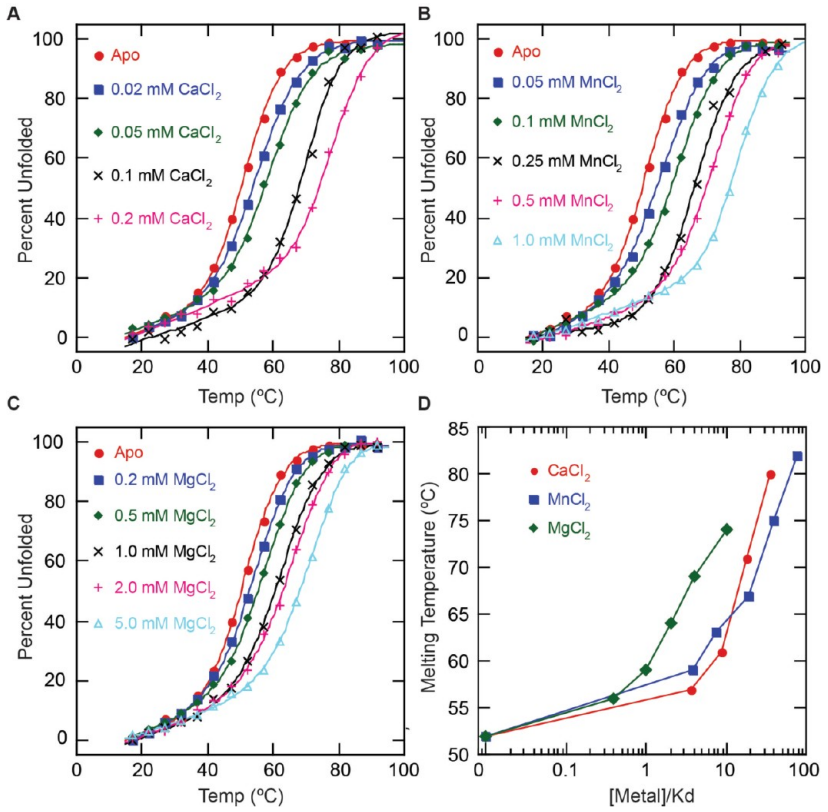

Figure 6. Stabilization of the N-CaM structure by metal ions. Melting profiles for N-CaM [in 10 mM Hepes (pH 7.5) and 3 M urea] at various metal ion concentrations were determined by monitoring the circular dichroism signal at 222 nm for (A) Ca^{2+}, (B) Mn^{2+}, and (C) Mg^{2+}. When the increase in melting temperature is plotted as a function of $[Me]/K_d$, the increase in stability induced by binding of each metal is similar as shown in panel D.

molecules in the crystal lattice, but not for the Ca^{2+}-binding loops where only Mn^{2+} ions are found. Apparently, the preference for tetrahedral ligand geometry makes Zn^{2+} incompatible with the ligand geometry in an EF-hand, which can accommodate metal ions in an octahedral or pentagonal bipyramid geometry only. Thus, Zn^{2+} ions cannot compete with Ca^{2+} for binding to EF-hand proteins.

Stabilization of the Closed-Domain Structure of N-CaM by Mg^{2+}. If Mg^{2+} does not induce domain opening in N-CaM then, does it have any effect on the structure at all? We have addressed this question by measuring the effects of increasing concentrations of Mg^{2+}, Mn^{2+}, and Ca^{2+} on the thermal denaturation of N-CaM. Binding of each of the metal ions tested increased the protein stability as reflected in the increase in unfolding temperature, consistent with the previous report.[46] To directly compare the effect of Mg^{2+} versus that of Ca^{2+}, we also included 3 M urea in the protein solution, thus lowering the temperature range for the unfolding transition. The increase in the unfolding temperature occurs in a different concentration range for each metal ion, with Ca^{2+} having the strongest effect (Figure 6a–c). However, when the melting temperature is plotted as a function of the $[Me]/K_d$ ratio, all three metal ions show similar effects on the stability of N-CaM (Figure 6d), despite the differences in the domain conformation. The Mg^{2+}-dependent stabilization of the closed-domain conformation has important functional implications. (1) In the absence of Ca^{2+}, it may prevent a partial activation of target enzymes that require the open-domain conformation of CaM, and (2) it may promote binding of CaM to the group of targets that have a preference for the closed-domain conformation, such as those involving the IQ domain. Such a preferential effect of Mg^{2+} on some model target–CaM interaction has been reported.[38]

DISCUSSION

The closed-domain, apo-like conformation is a common characteristic of the N-CaM structures presented here. The EF-hand loops are extended, and the Glu_{12} side chain, whose bidentate interaction with Ca^{2+} is critical for domain opening, does not directly contribute to Mg^{2+} or Mn^{2+} binding. Cumulatively, our data provide an explanation for the specific functional response of CaM to Ca^{2+} in the presence of Mg^{2+}. Unique structural features of the interaction of hydrated Mg^{2+} ion with N-CaM suggest a role for the hydration water in the mechanism of binding of metal to an EF-hand and the resultant conformational change.

Structural Basis for the Metal Ion-Dependent Functional Specificity in a Two-EF-Hand Domain. The structures of the Mg^{2+}–N-CaM complexes obtained in this work demonstrate that Mg^{2+} ions compete directly with Ca^{2+} in both EF-hand loops of N-CaM by engaging the same ligands in all but one coordinating position. Mg^{2+} fails to directly engage the two side-chain oxygen atoms of Glu_{12}, and the $-Z$ coordinating position is occupied by H_2O. In this respect, the Mg^{2+}–N-CaM interaction is similar to that found in site II of the Mg^{2+}–S100G complex.[27] The closed-domain conformation and the lack of contribution from Glu_{12} are consistent with the NMR data of Malmendal et al.,[17] with the lack of hydrophobic site exposure in CaM upon Mg^{2+} binding,[28] and with the lack of enzyme activation by the Mg^{2+}–CaM complex.[21] The high-

dx.doi.org/10.1021/bi300698h | Biochemistry 2012, 51, 6182–6194

Table 3. Geometry of Monodentate versus Bidentate Coordination of Mg^{2+}, Mn^{2+}, and Ca^{2+}

			bond angle (deg)		
metal ion	type of interaction	O−Me bond distance (Å)	C−O−Me	O−Me−O	PDB entry [resolution (Å)]
Ca^{2+}	monodentate	2.36 ± 0.05	138.0 ± 11.4	78.0 ± 2.4	1EXR (1.0)
	bidentate	2.50 ± 0.06	92.7 ± 2.7	52.5 ± 0.8	
Mg^{2+}	monodentate	2.08 ± 0.05	142.5 ± 14.6	90	3UCW (1.8)
	bidentate[a]	2.33	89.9	56.7	1Z2O (1.24)
Mn^{2+}	monodentate	2.17 ± 0.04	139.5 ± 10.8	90	3UCT (1.9)
	bidentate[a]	2.33	90.8	56.1	2W5T (1.6)

[a]For Mg^{2+} and Mn^{2+}, there are no examples of bidentate coordination among the published structures of EF-hand proteins. The examples given here were retrieved from the PDB using the MESPEUS server.[70]

resolution structures and data presented here offer a view into the underlying mechanism.

The lack of domain opening upon binding of Mg^{2+} to N-CaM can be attributed to several factors, all related in some ways to the smaller ionic radius of Mg^{2+} as compared to that of Ca^{2+}. It is possible that Mg^{2+} cannot engage the Glu_{12} bidentate ligand because the loop cannot contract sufficiently around the smaller Mg^{2+} ion. This, however, does not appear to play a role because in the structure of Mg^{2+}-bound parvalbumin[26] the Glu_{12} side chain is, in fact, involved in a direct monodentate interaction with Mg^{2+} (cf. Figure 3 of ref 12). Moreover, the monodentate interaction is retained even when the side chain is shortened by substitution of Asp for Glu_{12}.[47] Using molecular dynamics simulations, Cates et al.[48] have demonstrated a reversible switching from bidentate to monodentate interaction of Glu_{12} with the bound metal ion in parvalbumin in response to "alchemical" in silico conversion of Ca^{2+} into Mg^{2+}. The corresponding reduction from five to four oxygen atoms in the equatorial plane of the complex is necessary because the cavity formed by five oxygen atoms is too large for Mg^{2+} (cf. the discussion and Figure 3 of ref 12). The inability of Glu_{12} to engage in a bidentate interaction with Mg^{2+} (or Mn^{2+}) is also related to the geometric constraints on the bond lengths and bond angles for the bidentate type of carboxylate−metal ion interaction. The smaller the ionic radius, the closer the metal ion has to approach to the carboxylate oxygen atoms, which in turn constrains the bond angles. It is not possible to simultaneously satisfy the requirements for bond lengths and bond angles for a bidentate Mg^{2+}−carboxylate interaction. While there are examples in the Protein Data Bank of bidentate Mg^{2+} coordination by a carboxylate group (Table 3), these structures present a significantly distorted geometry, making their occurrences rare. The preference of Mg^{2+} ions for monodentate interaction with carboxylate group is even more striking for small molecule isolated ligands[41] and is well justified by the ab initio energy calculations showing that the monodentate Mg^{2+}−carboxylate interaction is >10 kcal/mol more stable than the bidentate interaction.[49]

What remains to be explained is why, in contrast to parvalbumin, in the Mg^{2+}−N-CaM complex the Glu_{12} side chain does not contribute any of its oxygen atoms to Mg^{2+} coordination, i.e., why a water molecule at the $-Z$ coordinating position is favored over the monodentate coordination by Glu_{12}. The explanation is in the different domain conformations of N-CaM and parvalbumin. In parvalbumin, the domain comprised of EF-hands II and III is fixed in the open conformation because of its strong interaction with nonfunctional EF-hand I. The EF-hand helices are in perpendicular orientation in which Glu_{12} always remains in a suitable position for interaction with a metal ion. In contrast, in N-CaM the movement of Glu_{12} (Glu31 and Glu67) into and out of the metal-coordinating position is structurally coupled to a change in the EF-hand interhelical angle associated with the Ca^{2+}-induced domain opening.[14,24] The energy of the interaction between Ca^{2+} and the two oxygen atoms of Glu_{12} must overcome the loss of interhelical hydrophobic contacts associated with domain opening (reviewed by Gifford et al.[15]). Thus, it is plausible that the inability of Glu_{12} in N-CaM to bind Mg^{2+} results from the lower overall binding energy; the K_d for binding of Mg^{2+} to N-CaM is only 0.45 mM as compared to 5.6 μM for Ca^{2+} (Table 2). However, this explanation is unsatisfactory in view of the fact that Mn^{2+}, which has an ionic radius similar to that of Mg^{2+} but binds N-CaM almost as strongly as Ca^{2+} (K_d = 13 μM), also does not engage Glu_{12}.

If neither the local metal−ligand interaction geometry nor the overall energy balance can provide an adequate explanation for our results, then we are left with the final possibility that the observed ligand−Mg^{2+} coordination in N-CaM is a result of some stereochemical constraints specific to the EF-hand. Such constraints are readily understood in light of the EF-hand β-scaffold mechanism, which attributes a special role to the invariant main-chain carbonyl group metal ligand in the $-Y$ coordinating position.[12] Unlike other ligands of the EF-hand Ca^{2+}-binding loop, the $-Y$ carbonyl oxygen is highly constrained because of the strong, polarized hydrogen bonds within the β-scaffold with the pair-mate Ca^{2+}-binding loop.[50] This, in turn, defines the position of the bound metal ion and, indirectly, limits the available conformational space for the other ligands. The ligands in the N-terminal part of the loop fold around the metal ion because of the flexibility of the main chain, whereas the C-terminal ligand (Glu_{12}) moves toward the metal ion together with the exiting helix, which in the case of Ca^{2+}, or any metal ion capable of accepting the bidentate coordination, results in the conformational transition. Bidentate coordination of Mg^{2+} is geometrically unfavorable, and a monodentate interaction is energetically insufficient to break the hydrophobic interhelical contacts. As a result, Glu_{12} is not engaged in the interaction and a water molecule occupies the vacant ligand position. In view of these considerations, we propose that the metal binding specificity of calmodulin, and more importantly its functional specificity, i.e., the ability to be activated specifically by Ca^{2+} but not by Mg^{2+}, is related primarily to the stereochemical constraints imposed on the metal ligands by the EF-hand β-scaffold. In view of the fact that all known EF-hand proteins appear to be composed of pairs of EF-hand motifs and preserve the EF-hand β-scaffold structure, it is likely that the rule mentioned above is applicable not only to CaM but to any EF-hand protein that has a sufficient affinity for Mg^{2+}.

dx.doi.org/10.1021/bi300698h | Biochemistry 2012, 51, 6182−6194

In the context of the conclusion described above, of particular interest is the potential effect of Mg^{2+} on the C-domain of CaM. Obtaining crystals of the Mg^{2+}-bound C-domain is technically more challenging because of its lower affinity for Mg^{2+} and higher affinity for Ca^{2+} as compared to the affinities for the N-domain.[37] However, on the basis of our circular dichroism-monitored melting profiles and bisANS fluorescence experiments, we conclude that, like in the N-domain, Mg^{2+} binding also stabilizes the closed conformation of the C-domain (Figure 3 of the Supporting Information). Although under physiological Mg^{2+} concentrations relatively little binding of Mg^{2+} to the C-domain of free CaM can be expected, the binding may be enhanced in the presence of CaM target molecules with a preference for the closed-domain conformation, such as the various IQ-domain-containing proteins.[38] Further studies are needed to fully evaluate the role of Mg^{2+} in the cellular function of CaM.

Potential Role of the Tightly Coordinated Water in the Metal-Dependent Conformational Transitions in EF-Hand Proteins. The unusual binding mode of the tetrahydrated Mg^{2+} ion in site II of N-CaM in the Mg^{2+}−N-CaM complex provides new insights into the mechanism of binding of metal ion to an EF-hand. As the Mn/Zn−N-CaM and Mg/Zn−N-CaM structures show, site II of N-CaM is perfectly competent to coordinate a dehydrated Mg^{2+} ion, or its equivalent Mn^{2+} ion, deep in the Ca^{2+}-binding loop, yet that is not the case in the Mg−N-CaM structure. In this structure, four of the six coordinating positions of the Mg^{2+} ion are still occupied by H_2O, which clearly is an intermediate state in the process of shedding the hydration water as a part of the binding mechanism. Mg^{2+} has an unusually high affinity for water, which is responsible for its generally weak interaction with most ligands and proteins. The transport number for Mg^{2+}, i.e., an average number of tightly associated water molecules that migrate through the solution as the cation diffuses, is 12−14 (cf. Table 1 of ref 51). Six of these water molecules coordinated octahedrally form the first hydration shell, which can be retained in the crystalline state.[52] The rate of water exchange from the first hydration shell is more than 1000-fold slower for Mg^{2+} than for Ca^{2+}.[53] This exceptionally strong interaction might be one of the reasons why we were able to capture the unusual state of $Mg^{2+}(H_2O)_4$ bound to an EF-hand. We believe that the structure represents a plausible intermediate state in the binding of Mg^{2+}, which occurs when a hydrated ion contacts the loop of an EF-hand (see the movie in the Supporting Information).

There are some striking features of the Mg^{2+}−N-CaM complex suggesting that binding of other metal ions, Ca^{2+} in particular, might occur through a similar intermediate state. CaM and other EF-hand proteins coordinate Ca^{2+} ions in a dehydrated form in which only one (or none at all) of the seven coordinating positions retains a water molecule. It is plausible that a transition from the fully hydrated ion in solution to the protein-bound dehydrated form involves some intermediate state(s) similar to that observed in the Mg−N-CaM structure. Such a state, if it exists, would facilitate the Ca^{2+}-induced conformational transition (see below). Here we will highlight the relevant observations. (1) Despite the presence of the hydration water, the interaction of $Mg^{2+}(H_2O)_4$ with site II of N-CaM is very strong mainly because of the double two-pronged, unusually short hydrogen bonds involving the side chains of Asp58 (hydrogen bond length of 2.66 ± 0.06 Å) and Glu67 (hydrogen bond length of 2.71 ± 0.06 Å). Although a similar complex of a hydrated Ca^{2+} ion would be significantly less stable because of the much faster solvent exchange rate for Ca^{2+} as compared to Mg^{2+},[53] it would likely be of sufficient stability to contribute to the transitions between the conformational states of CaM, which are estimated to occur on a microsecond or faster time scale.[54−56] (2) Because of the engagement of the equatorial ligands of the complex in the *Y* and −*Z* coordinating positions, the hydrated metal ion effectively bridges the opposite sides of the loop. The involvement of the key Glu_{12} appears to be of particular importance because it provides a direct link between the metal ion and the exiting helix. It is easy to envision that any change in the position or the hydration state of the bound metal ion in this dynamic complex would have an immediate effect on the exiting helix and could initiate the conformational transition. (3) At this early stage of metal−EF-hand interaction, the carbonyl oxygen of the *β*-scaffold (−*Y* position) is the only protein ligand whose interaction with the metal ion will remain unchanged in the final complex. Thus, as discussed above, the metal is already properly positioned for the loop to fold around it. (4) To accommodate the hydrated Mg^{2+}, the entering helix (helix C) had to be shifted away from the exiting helix (helix D) (Figure 3). This indicates that such a shift occurs readily without a significant perturbation of the remaining structure. There is evidence that such a shift in EF-hand I of N-CaM may be required for the conformational transition (see below). (5) The position of the bound $Mg^{2+}(H_2O)_4$ is very similar to that of Ca^{2+} in some EF-hand proteins that in the first loop position utilize a main-chain carbonyl oxygen as a ligand (Figure 2 of the Supporting Information; cf. ref 14). This type of Ca^{2+} coordination appears to be characteristic of the EF-hand proteins that do not undergo large conformational changes.

On the basis of the considerations mentioned above, it seems plausible that the binding of Ca^{2+} to EF-hand II of N-CaM may also involve a hydrated ion state analogous to the $Mg^{2+}(H_2O)_4$ state. Is it reasonable to extrapolate this conclusion to site I of N-CaM? The only change in the structure that would be required to accommodate a hydrated Ca^{2+} ion in site I of N-CaM is a small shift of helix A on the *Z* axis of the complex away from helix B. Recent atomistic multiscale simulations performed by Dupuis and Mousseau[57] provide support for such a process. These authors have investigated the mechanism of domain closing upon removal of Ca^{2+} from the holo state of N-domains of calmodulin and troponin C. The main contact between the ends of helices A and B in N-CaM is a highly conserved Phe residue (Phe19), whose bulky hydrophobic side chain has the unusual property of being more exposed to solvent in the closed-domain apo state than in the open-domain Ca^{2+} state. Dupuis and Mousseau have shown that expulsion of the Phe19 side chain (or its equivalent in troponin C) from the hydrophobic core is a necessary and limiting step in the domain closing transition.[57] Importantly, in each of their successful domain closing trajectories, the ends of helices A and B separated transiently to allow the Phe19 side chain to move out of the hydrophobic core (N. Mousseau and L. Dupuis, personal communication). The magnitude of such helix separation is similar to that we observe in site II of the Mg^{2+}−N-CaM complex. Thus, a transient adjustment of the domain structure that would be required for accommodation of the hydrated Ca^{2+} ion might facilitate the conformational transition by permitting the Phe19 side chain to move into the hydrophobic core. This is an attractive concept that adds a dynamic aspect to

dx.doi.org/10.1021/bi300698h | *Biochemistry* 2012, 51, 6182−6194

the EF-hand β-scaffold mechanism and warrants experimental verification.

Magnesium as a Modulator of Ca^{2+} Signaling in Cells. The free Mg^{2+} concentration in cells is buffered at a nearly constant level of ~1 mM. For that reason, Mg^{2+} is unlikely to have a direct regulatory role in cell signaling. However, it is clearly an important player in the Ca^{2+}−CaM signaling. As we have shown here, Mg^{2+} stabilizes the off state of CaM; thus, Mg^{2+} can act as a cellular break that counteracts the Ca^{2+} activation and facilitates switching off CaM when the Ca^{2+} concentration returns to resting levels. The effect of Mg^{2+} on CaM can be manifested in several ways. (a) Because of the Mg^{2+}/Ca^{2+} competition for the same binding sites, the apparent affinity of N-CaM for Ca^{2+} is decreased in the presence of Mg^{2+}; i.e., the titration curve is shifted to higher Ca^{2+} concentrations.[18] (b) In systems that involve fast Ca^{2+} transients, the Mg^{2+} dissociation rate may be a limiting factor; i.e., the extent of activation will be inversely related to the Mg^{2+} occupancy of N-CaM. Also under the conditions of partial activation when mixed Ca^{2+}/Mg^{2+} species may be formed, a different kinetic response may be expected.[18] (c) In view of the fact that some targets have a preference for the closed-domain conformation of CaM,[58] Mg^{2+} may affect the specificity of CaM and its distribution among the cellular targets.[38]

Ca^{2+} signaling in excitable cells such as neurons and myocytes has to be precise in terms of time, space, and amplitude, yet flexible enough to accommodate variable functional demands.[1,59] It appears that changes in Mg^{2+} concentration in response to various effectors[6,60−62] might provide the means to meet such variable demands by finely tuning the response of EF-hand-regulated systems, including various channel proteins.[63,64]

There are extensive studies documenting a correlation between dietary Mg^{2+} deficiency and various pathological conditions,[10] including cardiovascular diseases, hypertension, inflammation, asthma, metabolic syndrome, and many others.[65−69] Magnesium is the most abundant divalent metal ion in eukaryotic cells and plays many important cellular functions. However, none of these functions appear to be critically regulated by Mg^{2+} in the very narrow concentration range found in magnesium deficiency. We have put forward a hypothesis that EF-hand proteins might be involved, and their excessive activation at low Mg^{2+} might lead to impaired Ca^{2+} signaling, which in turn might be a contributing factor in some pathological conditions.[12] The structural information obtained in this work provides strong support for this hypothesis. Further studies are needed to test the applicability of the rules uncovered here to other EF-hand proteins and to characterize the effects of Mg^{2+} on various Ca^{2+} signaling pathways in cells.

■ ASSOCIATED CONTENT

Supporting Information

Determination of binding of Ca^{2+}, Mn^{2+}, and Mg^{2+} to N-CaM by isothermal titration calorimetry (Figure S1), comparison of EF-hand II of the Mg−N-CaM crystal with noncanonical EF-hand structures from calpain and calcyclin (Figure S2), stabilization of the closed-domain conformation in the C-terminal domain of CaM by Mg^{2+} (Figure S3), and putative steps in the binding of a hydrated Mg^{2+} ion $[Mg^{2+}(H_2O)_6]$ to site II of N-CaM (movie). This material is available free of charge via the Internet at http://pubs.acs.org.

Accession Codes

Coordinates and structure factors for the crystal structures of Mg/Zn−N-CaM, Mg−N-CaM, and Mn/Zn−N-CaM complexes are deposited in the Protein Data Bank as entries 3UCY, 3UCW, and 3UCT, respectively.

■ AUTHOR INFORMATION

Corresponding Author

*Boston Biomedical Research Institute, 64 Grove St., Watertown, MA 02472-2829. E-mail: grabarek@bbri.org. Telephone: (617) 658-7805. Fax: (617) 972-1753.

Funding

This work was supported by National Institutes of Health Grant HL91162.

Notes

The authors declare no competing financial interest.

■ ACKNOWLEDGMENTS

We thank Howard Robinson at the Brookhaven National Laboratory for collecting the synchrotron data at beamline X29 of the National Synchrotron Light Source (NSLS). We are grateful to Andrew Bohm, Celia Harrison, and Gretchen Meinke of Tufts University School of Medicine (Boston, MA) for their invaluable help with the initial screening of the crystals on their lab X-ray source. We thank Sam Lehrer, Franklin Fuchs, and Andrew Bohm for critical comments on the manuscript.

■ ABBREVIATIONS

CaM, recombinant human calmodulin; N-CaM, recombinant N-terminal fragment of calmodulin (residues 1−79); C-CaM, recombinant C-terminal fragment of calmodulin (residues 79−148); ITC, isothermal titration microcalorimetry; CD, circular dichroism.

■ REFERENCES

(1) Berridge, M. J., Lipp, P., and Bootman, M. D. (2000) The versatility and universality of calcium signalling. *Nat. Rev. Mol. Cell Biol. 1*, 11−21.

(2) Carafoli, E., Santella, L., Branca, D., and Brini, M. (2001) Generation, control, and processing of cellular calcium signals. *Crit. Rev. Biochem. Mol. Biol. 36*, 107−260.

(3) Clapham, D. E. (2007) Calcium signaling. *Cell 131*, 1047−1058.

(4) Romani, A., and Scarpa, A. (1992) Regulation of cell magnesium. *Arch. Biochem. Biophys. 298*, 1−12.

(5) Romani, A., and Scarpa, A. (1990) Hormonal control of Mg^{2+} transport in the heart. *Nature 346*, 841−844.

(6) Romani, A., Marfella, C., and Scarpa, A. (1993) Regulation of magnesium uptake and release in the heart and in isolated ventricular myocytes. *Circ. Res. 72*, 1139−1148.

(7) Fatholahi, M., LaNoue, K., Romani, A., and Scarpa, A. (2000) Relationship between total and free cellular Mg^{2+} during metabolic stimulation of rat cardiac myocytes and perfused hearts. *Arch. Biochem. Biophys. 374*, 395−401.

(8) Keenan, D., Romani, A., and Scarpa, A. (1996) Regulation of Mg^{2+} homeostasis by insulin in perfused rat livers and isolated hepatocytes. *FEBS Lett. 395*, 241−244.

(9) Romani, A. M., and Maguire, M. E. (2002) Hormonal regulation of Mg^{2+} transport and homeostasis in eukaryotic cells. *BioMetals 15*, 271−283.

(10) Seelig, M. S. (1980) *Magnesium deficiency in the pathogenesis of disease. Early roots of cardiovascular, skeletal and renal abnormalities*, Goldwater Memorial Hospital, New York University Medical Center, New York.

(11) Harkema, J. M., and Chaudry, I. H. (1992) Magnesium-adenosine triphosphate in the treatment of shock, ischemia, and sepsis. *Crit. Care Med. 20*, 263−275.
(12) Grabarek, Z. (2011) Insights into modulation of calcium signaling by magnesium in calmodulin, troponin C and related EF-hand proteins. *Biochim. Biophys. Acta 1813*, 913−921.
(13) Crivici, A., and Ikura, M. (1995) Molecular and structural basis of target recognition by calmodulin. *Annu. Rev. Biophys. Biomol. Struct. 24*, 85−116.
(14) Grabarek, Z. (2006) Structural basis for diversity of the EF-hand calcium-binding proteins. *J. Mol. Biol. 359*, 509−525.
(15) Gifford, J. L., Walsh, M. P., and Vogel, H. J. (2007) Structures and metal-ion-binding properties of the Ca^{2+}-binding helix-loop-helix EF-hand motifs. *Biochem. J. 405*, 199−221.
(16) Ohki, S. Y., Ikura, M., and Zhang, M. J. (1997) Identification of Mg^{2+}-binding sites and the role of Mg^{2+} on target recognition by calmodulin. *Biochemistry 36*, 4309−4316.
(17) Malmendal, A., Evenas, J., Thulin, E., Gippert, G. P., Drakenberg, T., and Forsen, S. (1998) When size is important. Accommodation of magnesium in a calcium binding regulatory domain. *J. Biol. Chem. 273*, 28994−29001.
(18) Malmendal, A., Linse, S., Evenas, J., Forsen, S., and Drakenberg, T. (1999) Battle for the EF-hands: Magnesium-calcium interference in calmodulin. *Biochemistry 38*, 11844−11850.
(19) Zhang, M., Tanaka, T., and Ikura, M. (1995) Calcium-induced conformational transition revealed by the solution structure of apo calmodulin. *Nat. Struct. Biol. 2*, 758−767.
(20) Tan, R. Y., Mabuchi, Y., and Grabarek, Z. (1996) Blocking the Ca^{2+}-induced conformational transitions in calmodulin with disulfide bonds. *J. Biol. Chem. 271*, 7479−7483.
(21) Chao, S. H., Suzuki, Y., Zysk, J. R., and Cheung, W. Y. (1984) Activation of calmodulin by various metal cations as a function of ionic radius. *Mol. Pharmacol. 26*, 75−82.
(22) Kretsinger, R. H., and Nockolds, C. E. (1973) Carp muscle calcium binding protein. II. Structure determination and general description. *J. Biol. Chem. 248*, 3313−3326.
(23) Strynadka, N. C. J., and James, M. N. G. (1989) Crystal structures of the helix-loop-helix calcium-binding proteins. *Annu. Rev. Biochem. 58*, 951−998.
(24) Grabarek, Z. (2005) Structure of a trapped intermediate of calmodulin: Calcium regulation of EF-hand proteins from a new perspective. *J. Mol. Biol. 346*, 1351−1366.
(25) Gagne, S. M., Li, M. X., and Sykes, B. D. (1997) Mechanism of direct coupling between binding and induced structural change in regulatory calcium binding proteins. *Biochemistry 36*, 4386−4392.
(26) Declercq, J. P., Tinant, B., Parello, J., and Rambaud, J. (1991) Ionic interactions with parvalbumins. Crystal structure determination of pike 4.10 parvalbumin in four different ionic environments. *J. Mol. Biol. 220*, 1017−1039.
(27) Andersson, M., Malmendal, A., Linse, S., Ivarsson, I., Forsen, S., and Svensson, L. A. (1997) Structural basis for the negative allostery between Ca^{2+}- and Mg^{2+}-binding in the intracellular Ca^{2+}-receptor calbindin D9k. *Protein Sci. 6*, 1139−1147.
(28) Follenius, A., and Gerard, D. (1984) Fluorescence investigations of calmodulin hydrophobic sites. *Biochem. Biophys. Res. Commun. 119*, 1154−1160.
(29) Doering, D. S., and Matsudaira, P. (1996) Cysteine scanning mutagenesis at 40 of 76 positions in villin headpiece maps the F-actin binding site and structural features of the domain. *Biochemistry 35*, 12677−12685.
(30) Wiseman, T., Williston, S., Brandts, J. F., and Lin, L. N. (1989) Rapid measurement of binding constants and heats of binding using a new titration calorimeter. *Anal. Biochem. 179*, 131−137.
(31) Meyer, D. F., Mabuchi, Y., and Grabarek, Z. (1996) The role of Phe-92 in the Ca^{2+}-induced conformational transition in the C-terminal domain of calmodulin. *J. Biol. Chem. 271*, 11284−11290.
(32) Otwinowski, Z., and Minor, W. (1997) Processing of X-ray diffraction data collected in oscillation mode. *Methods Enzymol. 276*, 307−326.
(33) Collaborative Computational Project, Number 4 (1994) The CCP4 suite: Programs for protein crystallography. *Acta Crystallogr. D50*, 760−763.
(34) Adams, P. D., Grosse-Kunstleve, R. W., Hung, L. W., Ioerger, T. R., McCoy, A. J., Moriarty, N. W., Read, R. J., Sacchettini, J. C., Sauter, N. K., and Terwilliger, T. C. (2002) PHENIX: Building new software for automated crystallographic structure determination. *Acta Crystallogr. D58*, 1948−1954.
(35) Terwilliger, T. C., Grosse-Kunstleve, R. W., Afonine, P. V., Moriarty, N. W., Adams, P. D., Read, R. J., Zwart, P. H., and Hung, L.-W. (2008) Iterative-build OMIT maps: Map improvement by iterative model building and refinement without model bias. *Acta Crystallogr. D64*, 515−524.
(36) Emsley, P., and Cowtan, K. (2004) Coot: Model-building tools for molecular graphics. *Acta Crystallogr. D60*, 2126−2132.
(37) Tsai, M. D., Drakenberg, T., Thulin, E., and Forsen, S. (1987) Is the binding of magnesium(II) to calmodulin significant? An investigation by magnesium-25 nuclear magnetic resonance. *Biochemistry 26*, 3635−3643.
(38) Martin, S. R., Masino, L., and Bayley, P. M. (2000) Enhancement by Mg^{2+} of domain specificity in Ca^{2+}-dependent interactions of calmodulin with target sequences. *Protein Sci. 9*, 2477−2488.
(39) Warren, J. T., Guo, Q., and Tang, W. J. (2007) A 1.3-Å structure of zinc-bound N-terminal domain of calmodulin elucidates potential early ion-binding step. *J. Mol. Biol. 374*, 517−527.
(40) Shannon, R. D. (1976) Revised effective ionic radii and systematic studies of interatomic distances in halides and chalcogenides. *Acta Crystallogr. A32*, 751−767.
(41) Carrell, C. J., Carrell, H. L., Erlebacher, J., and Glusker, J. P. (1988) Structural aspects of metal-ion carboxylate interactions. *J. Am. Chem. Soc. 110*, 8651−8656.
(42) Harding, M. M. (2006) Small revisions to predicted distances around metal sites in proteins. *Acta Crystallogr. D62*, 678−682.
(43) Delville, A., Grandjean, J., Laszlo, P., Gerday, C., Brzeska, H., and Drabikowski, W. (1980) Sodium-23 nuclear magnetic resonance as an indicator of sodium binding to calmodulin and tryptic fragments, in relation to calcium content. *Eur. J. Biochem. 109*, 515−522.
(44) Moroz, O. V., Blagova, E. V., Wilkinson, A. J., Wilson, K. S., and Bronstein, I. B. (2009) The crystal structures of human S100A12 in apo form and in complex with zinc: New insights into S100A12 oligomerisation. *J. Mol. Biol. 391*, 536−551.
(45) Irving, H., and Williams, R. J. P. (1953) The stability of transition-metal complexes. *J. Chem. Soc.,*, 3192−3210.
(46) Brzeska, H., Venyaminov, S. V., Grabarek, Z., and Drabikowski, W. (1983) Comparative studies on thermostability of calmodulin, skeletal muscle troponin C and their tryptic fragments. *FEBS Lett. 153*, 169−173.
(47) Cates, M. S., Berry, M. B., Ho, E. L., Li, Q., Potter, J. D., and Phillips, G. N., Jr. (1999) Metal-ion affinity and specificity in EF-hand proteins: Coordination geometry and domain plasticity in parvalbumin. *Structure in Folding and Design 7*, 1269−1278.
(48) Cates, M. S., Teodoro, M. L., and Phillips, G. N., Jr. (2002) Molecular mechanisms of calcium and magnesium binding to parvalbumin. *Biophys. J. 82*, 1133−1146.
(49) Deerfield, D. W., II, Fox, D. J., Head-Gordon, M., Hiskey, R. G., and Pedersen, L. G. (1995) The first solvation shell of magnesium ion in a model protein environment with formate, water, and X-NH3, H2S, imidazole, formaldehyde, and chloride as ligands: An ab initio study. *Proteins 21*, 244−255.
(50) Biekofsky, R. R., Martin, S. R., Browne, J. P., Bayley, P. M., and Feeney, J. (1998) Ca^{2+} coordination to backbone carbonyl oxygen atoms in calmodulin and other EF-hand proteins: ^{15}N chemical shifts as probes for monitoring individual-site Ca^{2+} coordination. *Biochemistry 37*, 7617−7629.
(51) Maguire, M. E., and Cowan, J. A. (2002) Magnesium chemistry and biochemistry. *BioMetals 15*, 203−210.

(52) Johnson, C. (1965) X-ray crystal analysis of the substrates of aconitase. V. Magnesium citrate decahydrate $[Mg(H_2O)_6]$-$[MgC_6H_5O_7(H_2O)]_2 \cdot 2H_2O$. *Acta Crystallogr. 18*, 1004−1018.
(53) Diebler, H., Eigen, M., Ilgenfritz, G., Maass, G., and Winkler, R. (1969) Kinetics and mechanism of reactions of main group metal ions with biological carriers. *Pure Appl. Chem. 20*, 93−115.
(54) Evenas, J., Malmendal, A., Thulin, E., Carlstrom, G., and Forsen, S. (1998) Ca^{2+} binding and conformational changes in a calmodulin domain. *Biochemistry 37*, 13744−13754.
(55) Evenas, J., Forsen, S., Malmendal, A., and Akke, M. (1999) Backbone dynamics and energetics of a calmodulin domain mutant exchanging between closed and open conformations. *J. Mol. Biol. 289*, 603−617.
(56) Evenas, J., Malmendal, A., and Akke, M. (2001) Dynamics of the transition between open and closed conformations in a calmodulin C-terminal domain mutant. *Structure 9*, 185−195.
(57) Dupuis, L., and Mousseau, N. (2012) Understanding the EF-hand closing pathway using non-biased interatomic potentials. *J. Chem. Phys. 136*, 035101.
(58) Jurado, L. A., Chockalingam, P. S., and Jarrett, H. W. (1999) Apocalmodulin. *Physiol. Rev. 79*, 661−682.
(59) Berridge, M. J., Bootman, M. D., and Lipp, P. (1998) Calcium: A life and death signal. *Nature 395*, 645−648.
(60) Romani, A. M., and Scarpa, A. (2000) Regulation of cellular magnesium. *Front. Biosci. 5*, D720−D734.
(61) Romani, A. M. (2011) Cellular magnesium homeostasis. *Arch. Biochem. Biophys. 512*, 1−23.
(62) Brocard, J. B., Rajdev, S., and Reynolds, I. J. (1993) Glutamate-induced increases in intracellular free Mg^{2+} in cultured cortical neurons. *Neuron 11*, 751−757.
(63) Lee, A., Zhou, H., Scheuer, T., and Catterall, W. A. (2003) Molecular determinants of Ca^{2+}/calmodulin-dependent regulation of $Ca_v2.1$ channels. *Proc. Natl. Acad. Sci. U.S.A. 100*, 16059−16064.
(64) Brunet, S., Scheuer, T., Klevit, R., and Catterall, W. A. (2005) Modulation of $Ca_V1.2$ channels by Mg_{2+} acting at an EF-hand motif in the COOH-terminal domain. *J. Gen. Physiol. 126*, 311−323.
(65) Rayssiguier, Y., Mbega, J. D., Durlach, V., Gueux, E., Durlach, J., Giry, J., Dalle, M., Mazur, A., Laurant, P., and Berthelot, A. (1992) Magnesium and blood pressure. I. Animal studies. *Magnesium Res. 5*, 139−146.
(66) Touyz, R. M. (2003) Role of magnesium in the pathogenesis of hypertension. *Mol. Aspects Med. 24*, 107−136.
(67) Touyz, R. M. (2004) Magnesium in clinical medicine. *Front. Biosci. 9*, 1278−1293.
(68) Weglicki, W., Quamme, G., Tucker, K., Haigney, M., and Resnick, L. (2005) Potassium, magnesium, and electrolyte imbalance and complications in disease management. *Clin. Exp. Hypertens. 27*, 95−112.
(69) Mazur, A., Maier, J. A., Rock, E., Gueux, E., Nowacki, W., and Rayssiguier, Y. (2007) Magnesium and the inflammatory response: Potential physiopathological implications. *Arch. Biochem. Biophys. 458*, 48−56.
(70) Hsin, K., Sheng, Y., Harding, M. M., Taylor, P., and Walkinshaw, M. D. (2008) MESPEUS: A database of the geometry of metal sites in proteins. *J. Appl. Crystallogr. 41*, 963−968.
(71) DeLano, W. L. (2002) *The PyMOL Molecular Graphics System*, DeLano Scientific, Palo Alto, CA.